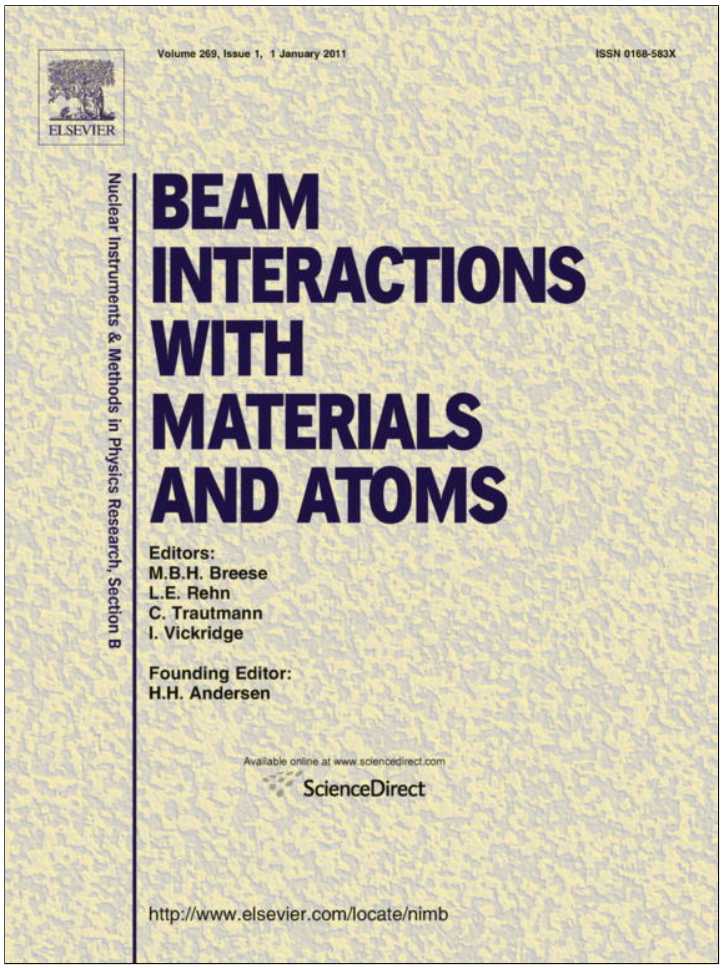

(This is a sample cover image for this issue. The actual cover is not yet available at this time.)

Nuclear Instruments and Methods in Physics Research B 269 (2011) 1431–1443

Contents lists available at ScienceDirect

Nuclear Instruments and Methods in Physics Research B

journal homepage: www.elsevier.com/locate/nimb

Simulations of thermally transferred OSL signals in quartz: Accuracy and precision of the protocols for equivalent dose evaluation

Vasilis Pagonis [a,*], Grzegorz Adamiec [b], C. Athanassas [c], Reuven Chen [d], Atlee Baker [a], Meredith Larsen [a], Zachary Thompson [a]

[a] Physics Department, McDaniel College, Westminster, MD 21157, USA
[b] Silesian University of Technology, Institute of Physics, GADAM Centre of Excellence, ul. Krzywoustego 2, 44-100 Gliwice, Poland
[c] Laboratory of Archaeometry, Institute of Materials Science, N.C.S.R. 'Demokritos', Aghia Paraskevi, Athens153 10, Greece
[d] Raymond and Beverly Sackler School of Physics and Astronomy, Tel-Aviv University, Tel-Aviv 69978, Israel

ARTICLE INFO

Article history:
Received 11 November 2010
Received in revised form 30 March 2011
Available online 6 April 2011

Keywords:
Thermoluminescence (TL)
Optically stimulated luminescence (OSL)
Equivalent dose estimation
Quartz
Retrospective dosimetry
Authenticity testing
Accident dosimetry
Kinetic rate equations
SAR technique
TT-OSL

ABSTRACT

Thermally-transferred optically stimulated luminescence (TT-OSL) signals in sedimentary quartz have been the subject of several recent studies, due to the potential shown by these signals to increase the range of luminescence dating by an order of magnitude. Based on these signals, a single aliquot protocol termed the ReSAR protocol has been developed and tested experimentally. This paper presents extensive numerical simulations of this ReSAR protocol. The purpose of the simulations is to investigate several aspects of the ReSAR protocol which are believed to cause difficulties during application of the protocol. Furthermore, several modified versions of the ReSAR protocol are simulated, and their relative accuracy and precision are compared. The simulations are carried out using a recently published kinetic model for quartz, consisting of 11 energy levels. One hundred random variants of the natural samples were generated by keeping the transition probabilities between energy levels fixed, while allowing simultaneous random variations of the concentrations of the 11 energy levels. The relative intrinsic *accuracy* and *precision* of the protocols are simulated by calculating the equivalent dose (ED) within the model, for a given natural burial dose of the sample. The complete sequence of steps undertaken in several versions of the dating protocols is simulated. The relative intrinsic *precision* of these techniques is estimated by fitting Gaussian probability functions to the resulting simulated distribution of ED values. New simulations are presented for commonly used OSL sensitivity tests, consisting of successive cycles of sample irradiation with the same dose, followed by measurements of the sensitivity corrected L/T signals. We investigate several experimental factors which may be affecting both the intrinsic precision and intrinsic accuracy of the ReSAR protocol. The results of the simulation show that the four different published versions of the ReSAR protocol can reproduce accurately the natural doses in the range 0–400 Gy with approximately the same intrinsic precision and accuracy of ~1–5%. However, these protocols underestimate doses above 400 Gy; possible sources of this underestimation are investigated. Two possible explanations are suggested for the modeled underestimations, possible thermal instability of the TT-OSL traps, and the presence of thermally unstable medium OSL components in the model.

1. Introduction

Thermally-transferred optically stimulated luminescence (TT-OSL) signals in sedimentary quartz have been the subject of several recent studies, due to the possibility of using these signals to increase the range of luminescence dating by an order of magnitude [33,34,35]. The TT-OSL signal is thought to consist of two components, a dose dependent component originating in a "source TT-OSL trap", and a second component which may or may not be dose independent, which is termed the basic transferred OSL (BT-OSL). Wang et al. [35] developed a single aliquot measurement protocol which was applied to several samples of Chinese loess. In analogy to the well-established SAR protocol, the OSL responses to a test dose are used to correct the TT-OSL signals for sensitivity changes occurring during the dating protocol [36]. This single aliquot protocol based on TT-OSL signals has been termed as ReSAR protocol and is the subject of this paper.

Perhaps the main drawback of the ReSAR protocol is its complexity, which makes it very time consuming from the experimental point of view, especially that usually high regeneration doses are used. Several researchers have applied the ReSAR protocol to different sedimentary quartz samples, and suggested that it may

* Corresponding author. Tel.: +1 410 857 2481; fax: +1 410 386 4624.
E-mail address: vpagonis@mcdaniel.edu (V. Pagonis).

0168-583X/$ - see front matter © 2011 Elsevier B.V. All rights reserved.
doi:10.1016/j.nimb.2011.03.026

possible to improve its accuracy by making modifications, and perhaps even to simplify the protocol [32,26,30,15,2]. Some of the problems associated with the protocol are non-zero TT-OSL intensity values obtained for zero dose regeneration and poor recycling ratios. The work of Tsukamoto et al. [32], Porat et al. [26], Stevens et al. [30] and Adamiec et al. [2] is discussed in detail in later section of this paper. In a recently published study Kim et al. [15] studied the TT-OSL signals from seven loess-like fine grained samples from Korea, and examined the various procedures for separating the ReOSL and BT-OSL components. In another notable study Athanassas and Zacharias [3] studied raised marine sequences in the South-West coast of Greece during Upper Quaternary. These authors tested the suitability of the ReSAR protocol by applying it to coarse-grained quartz aliquots from nearshore outcrops. They studied the TT-OSL signal characteristics, dose response and sensitivity changes, recovery of known laboratory doses and the signal's bleachability by sunlight. The accuracy of the Re-OSL dates calculated for natural samples was compared with dates obtained from the SAR-OSL protocol.

It is believed that the mechanism by which TT-OSL is produced is a single transfer mechanism, in which electrons are thermally transferred from a source trap into the OSL trap and are subsequently measured as a TT-OSL signal. Numerical modeling studies and associated experimental work have provided strong support for this single transfer mechanism [1,23,22,21]. In a recently published study Adamiec et al. [2] carried out a detailed experimental study in order to identify the traps that are sources of the TT-OSL signal. During their study they determined the thermal stability of the signals by using TL peaks associated with the TT-OSL signals. They used the information on thermal stability to develop a more appropriate ReSAR protocol that was tested using sensitivity tests.

The purpose of this paper is to investigate several aspects of the ReSAR protocol using the recently published model by [22,23]. The main goals are to investigate the various factors affecting both the intrinsic precision and the accuracy of the ReSAR protocol, and to identify possible sources for some of the difficulties encountered while using this protocol in experimental studies.

2. Description of the model

The simulations in this paper are carried out using the comprehensive quartz model developed by Pagonis et al. [22–24]. This model is based on a previous model by Bailey [4] that was developed on the basis of empirical data. Fig. 1 shows the energy level diagram for the model used in this paper. The set of differential equations and the choice of parameters were presented recently by Pagonis et al. [22,23], and will not be repeated here. For easy reference we briefly describe here the various energy levels in the model, as well as present the values of the kinetic parameters in Table 1.

The original model by Bailey [4] consists of 5 electron traps and 4 hole centers, and has been used successfully to simulate a wide variety of TL and OSL phenomena in quartz. This model was expanded by Pagonis et al. [22,23] to include two additional levels, as described below. Level 1 in the model represents a shallow electron trapping level, which gives rise to a TL peak at ~100 °C with a heating rate of 5 K/s. The TL and OSL signal from this trap do not play a major role in the TT-OSL protocols simulated in this paper. Level 2 represents a generic "230 °C TL" trap, typically found in many quartz samples. The TL signal from this trap has been used successfully in several comprehensive experimental dating studies [7,8,14,9,13]. Levels 3 and 4 are usually termed the fast and medium OSL components and they yield TL peaks at ~330 °C as well as giving rise to OSL signals. The OSL from levels 3 and 4 forms the basis of the very precise and accurate SAR protocols [36]. The model does not contain any of the slow OSL components which are known to be present in quartz, and which were incorporated in later versions of the model [5]. Level 5 is a deep electron center which is considered thermally disconnected. Levels 6 and 7 are thermally unstable, non-radiative recombination centers (also termed "hole reservoirs"). These two levels play a crucial role in the predose (dose dependent) sensitization mechanism which forms the basis of the predose dating technique.

Level 8 is a thermally stable, radiative recombination center often termed the "luminescence center" (L). Level 9 is a thermally stable, non-radiative recombination center termed a "killer" center (K). Levels 10 and 11 are the two new levels added to the original Bailey model by Pagonis et al. [22,23], and were introduced in order to simulate the experimentally observed thermally transferred OSL (TT-OSL) signals and basic transferred OSL (BT-OSL) signals [33,34]. Level 10 in the model represents the source trap for the TT-OSL signal and is a slightly less thermally stable trap with high dose saturation. It is assumed that electrons are thermally transferred into the fast component trap (level 3) from level 10. This trap (level 10) is assumed to be emptied optically in nature by long sunlight exposure. Level 11 is believed to contribute most of the BT-OSL signal in quartz; these traps are believed to be much less light-sensitive than level 10, and also are thought to be more thermally stable than either level 3 or level 10 [2,22,23].

The kinetic parameters in Table 1 are as defined by Bailey [4]; N_i are the concentrations of electron traps or hole centers (cm^{-3}), n_i

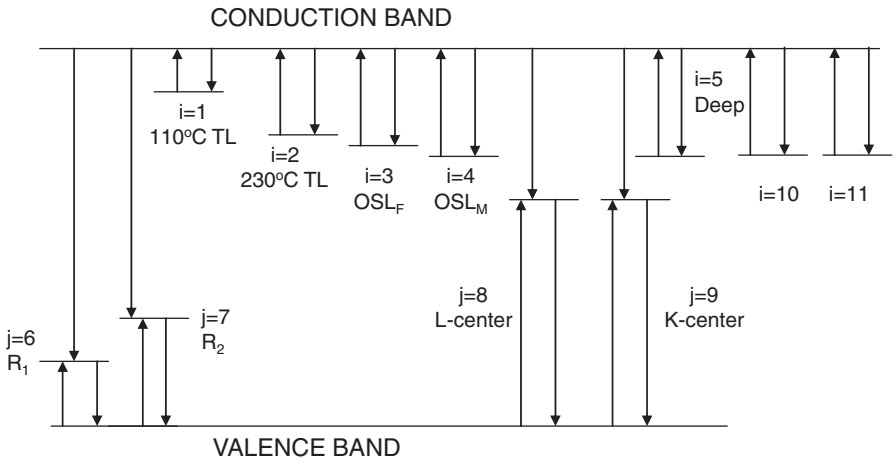

Fig. 1. Schematic diagram of the comprehensive quartz model of Pagonis et al. [22,23]) used in this paper. The two levels labeled $i = 10$ and 11 were added to the original model by Bailey [4], and are believed to play a fundamental role in the production of the TT-OSL signals in quartz.

Table 1
The parameters of [22,23] are shown together with modified values for N_{10} and N_{11} introduced in the present simulations shown in bold. The modified values are the experimental parameters E and s reported by Adamiec et al. [2].

	Ni cm^{-3}	E_i eV	s_i s^{-1}	A_i B_i $cm^3\ s^{-1}$	θ_{0i} s^{-1}	E_ith eV
1	1.5e7	0.97	5e12	1e-8	0.75	0.1
2	1e7	1.55	5e14	1e-8	0	0
3	4e7	1.73	6.5e13	5e-9	6	0.1
4	2.5e8	1.8	1.5e13	5e-10	4.5	.13
5	5e10	2	1e10	1e-10	0	0
6	3e8	1.43	5e13	5e-7 5e-9	0	0
7	1e10	1.75	5e14	1e-9 5e-10	0	0
8	3e10	5	1e13	1e-10 1e-10	0	0
9	1.2e12	5	1e13	1e-14 3e-10	0	0
10	5e9	**1.46**	**1.65e11**	1e-11	0.01	0.2
11	4e9	**1.72**	**2.9e13**	6e-12	0	0

are the concentrations of trapped electrons or holes (cm^{-3}), s_i are the frequency factors (s^{-1}), E_i are the electron trap depths below the conduction band or hole trap depths above the valence band (eV), A_i (i = 1...5, and i = 10 and 11) are the conduction band to electron trap transition probability coefficients ($cm^3\ s^{-1}$), A_j (j = 6...9) are the valence band to hole trap transition probability coefficient ($cm^3\ s^{-1}$), valence band to trap transition probability coefficients ($cm^3\ s^{-1}$) and B_j (j = 6...9) are the conduction band to hole center transition probability coefficients ($cm^3\ s^{-1}$). Other parameters related to the photoionization cross-sections of the optically sensitive traps are the photo-eviction constant θ_{0i} (s^{-1}) at $T = \infty$, the thermal assistance energy E_ith (eV). The numerical values given in Table 1 are those given in Table 2 of Pagonis et al. [22,23], with one important change; we use the experimental values of the kinetic parameters reported by Adamiec et al. [2] for levels 10 and 11 in the model. This choice is discussed in some detail in a subsequent section.

In all simulations presented in this paper we simulate the irradiation of quartz samples in nature as realistically as possible, by assuming that the quartz sample has received burial doses with a natural dose rate of 3×10^{-11} Gy/s. By contrast, laboratory simulations are simulated at a much higher dose rate of 0.1–1 Gy/s.

In the rest of this paper it will be demonstrated that by using the set of parameters in Table 1, it is possible to simulate the complete experimental protocols for different versions of the ReSAR dating techniques. Tables 2 and 3 show in schematic form the simulation steps for calculating the ED using the ReSAR and SAR-OSL dating techniques respectively. Tables 4–6 show in schematic form the simulation steps in three recently published modified versions of the ReSAR protocol, namely the protocol of Porat et al. [26], Stevens et al. [30] and Adamiec et al. [2].

There are additional relaxation steps in the simulations which are not shown explicitly in Tables 2–6. Specifically after each excitation stage in the simulations a relaxation period is introduced in which the temperature of the sample is kept constant at room temperature for 1 s after the excitation has stopped (R = 0), and during which the concentrations of n_c and n_v decay to negligible values. After each heating cycle the model simulates a cooling-down period with a constant cooling rate of $\beta = -5$°C s^{-1}. A linear heating rate $\beta = 5$°C s^{-1} is assumed during the simulation of the TL glow curves, so that $T = T_0 + \beta t$ and R = 0 during the readout stage. During irradiation a value of $R = 5 \times 10^7$ pairs/s is used to simulate an irradiation dose rate of 1 Gy/s. The simulated TT-OSL signals in our simulations are approximately two orders of magnitude weaker than the corresponding simulated OSL signals. This is consistent with several experimental studies of the TT-OSL phenomenon.

3. Simulation of random natural variations in quartz samples

Our simulation method is similar to the published work by Bailey [5]. Specifically we simulate the experimentally observed variability in TL and OSL characteristics of quartz by assuming that all the fundamental transition probabilities in the model remain constant, while trap concentrations (parameters N_1, $N_2 \ldots N_{11}$ in Table 1) are allowed to vary randomly within arbitrary limits of ±80% from the values shown in Table 1. As discussed in [5], some variation of the transition probabilities may also be present in natural samples, but this variation is expected to be relatively insignificant.

We use the parameters of the comprehensive model of [22,23] as our "standard" quartz model, with the experimental values of the kinetic parameters found by Adamiec et al. [2] for levels 10 and 11 in the model. This is discussed in the next section. N = 300 versions of the parameters were generated by randomly selecting electron and hole concentration values within ±80% of the original values, using uniformly distributed random numbers. For each of these variants the full sequence of irradiation and thermal history of the natural samples were simulated, and the luminescence dating protocols were simulated in order to obtain an estimate of their relative accuracy and precision. The complete sequence of the simulated protocols is shown in Tables 2–6. Even

Table 2
The simulation steps for the ReSAR technique of Wang et al. [35]. A single aliquot is used for all measurements. Steps 1–4 are a simulation of a "natural" quartz sample according to Bailey [4], with a variable natural burial dose D. In some of the simulations the sample is optically bleached by adding step 5. Also in some of the simulations the additional step 21 is added, as suggested by Tsukamoto et al. [32].

1 Geological dose irradiation of 1000 Gy at 1 Gy/s
2 Geological time – heat to 350 °C
3 Illuminate for 100 s at 200 °C
4 Burial dose – D at 20 °C at 3×10^{-11} Gy/s
5 In some simulations add the following step:
Optical Bleaching of sample: blue stimulation at 125 °C for 2000 s
6 Regenerated dose D_i at 20 °C and at 1 Gy/s
7 Preheat to 260 °C for 10 s
8 Blue stimulation at 125 °C for 270 s
9 Preheat to 260 °C for 10 s
10 Blue stimulation at 125 °C for 90 s ($L_{TT\text{-}OSL}$)
11 Test dose TD = 7 Gy
12 Preheat to 220 °C for 20 s
13 Blue stimulation at 125 °C for 90 s ($T_{TT\text{-}OSL}$)
14 Anneal to 300 °C for 10 s
15 Blue stimulation at 125 °C for 90 s
16 Preheat at 260 °C for 10 s
17 Blue stimulation at 125 °C for 90 s (LBT-OSL)
18 Test dose TD = 7 Gy
19 Preheat to 220 °C for 20 s
20 Blue stimulation at 125 °C for 90 s (TBT-OSL)
21 In some simulations, the following step is added:
Blue stimulation at 280 °C for 90 s, as suggested by Tsukamoto et al. [32].
Repeat steps 6–21 for a sequence of different regenerative doses e.g. D_i = (0, 500, 1000, 1500, 0, 500 Gy) to reconstruct the dose response curve. Estimate ED using interpolation.

Table 3
The simulation steps for the SAR-OSL technique. A single aliquot is used for all measurements.

1–4 Steps 1–4 are the same as in Table 2
5 Irradiate sample with dose Di
6 Preheat 10 s at 260oC
7 Blue OSL for 100 s at 125 °C – Record OSL (0.1 s) signal (L)
8 Test dose TD = 5 Gy
9 Cutheat 20 s at 220 °C
10 Blue OSL for 100 s at 125 °C – Record OSL (0.1 s) signal (T)
Repeat steps 5–10 for a sequence of different regenerative doses e.g. D_i = (0, 500, 1000, 1500, 0, 500 Gy) to reconstruct the dose response curve L/T vs dose. Estimate ED using interpolation.

Table 4
The simulation steps for the Porat et al. [24] protocol.

1–4 Steps 1–4 are the same as in Table 2
5 Irradiate sample with dose Di
6 Preheat at 200–260 °C for 10 s
7 Blue stimulation for 300 s at 125 °C
8 TT-OSL inducing preheat at 260 °C for 10 s
9 CW-OSL for 100 s at 125°C (Lx-signal)
10 Irradiation with test dose (~5 Gy)
11 Pre heat at 220 °C for 10 s
12 CW-OSL for 100 s at 125°C (Tx-signal)
13 Thermal treatment of 300 °C for 100 s
14 Go to step 5

Table 5
The simulation steps for the Stevens et al. [30] protocol.

1–4 Steps 1–4 are the same as in Table 2
5 Irradiate sample with dose D_i
6 Preheat at 260 °C for 10 s
7 OSL for 60 s at 125 °C
8 TT-OSL inducing preheat at 260°C for 10 s
9 CW-OSL for 60 s at 125°C (L-signal)
10 **High temperature bleaching step: OSL for 400 s at 280 °C**
11 Irradiation with test dose (23 Gy)
12 Preheat at 220 °C for 10 s
13 CW-OSL for 60 s at 125 °C (T-signal)
14 **High temperature bleaching step: OSL for 400 s at 290 °C**
15 Go to step 5

Table 6
The simulation steps for the Adamiec et al. [2] protocol.

1–4 Steps 1–4 are the same as in Table 2
5 Irradiate sample with dose D_i
6 Preheat at 260 °C for 10 s
7 LM-OSL for 200 s at 125 °C
8 TT-OSL inducing preheat at 260 °C for 10 s
9 CW-OSL for 100 s at 125 °C (Lx-signal)
10 Irradiation with test dose (~5 Gy)
11 Pre heat at 220 °C for 10 s
12 CW-OSL for 100 s at 125 °C (Tx-signal)
13 Thermal treatment of 350 °C for 200 s
14 Go to step 5

The sequence of doses D_i in step 5 are: no irradiation, irradiation with regeneration doses D_1, D_2, D_3, no irradiation and one of the previous regeneration doses for recycling ratio.

though our approach in this paper is similar to that of Bailey [5], our goals are different. We are interested in a comparative study of the various factors affecting the accuracy and precision of the simulated ReSAR dating protocols. Furthermore, we simulate the accuracy and precision of the dose responses of the TT-OSL and OSL signals, as well as present new simulations of sensitivity changes occurring during the various protocols.

An initial set of simulations was carried out using $N = 300$ random concentration variants, and the results were compared with those obtained when using only $N = 100$ variants. Comparison of the $N = 300$ and $N = 100$ results showed a very small improvement of less than 0.5% in the precision of the simulated results, while the corresponding accuracy of the simulations remained unaffected. On the basis of these initial results, it was decided to carry out the rest of the simulations for $N = 100$ natural variants of the sample, for the sake of saving very significant amounts of computation time.

The computer code is written in *Mathematica*, and typical running times for 100 variations of the SAR-OSL techniques are ~40 min on a PC. It was found necessary to use a solver for "stiff" differential equations in several of the simulations, and the *Mathematica* software switched automatically between a stiff and non-stiff Runge–Kutta solver whenever necessary.

An important point needs to be made about the choice of ±80% variation used to produce the 100 variants of the model. As discussed in Bailey [5], the ±80% variation limit is chosen rather arbitrarily, and there is no compelling reason for choosing this specific value. However, one can make a reasonable argument for choosing this level of variation as follows; we know from experimental work that the SAR protocol for well behaved quartz samples can achieve accuracy and precision as good as 1% in many cases. The *intrinsic* accuracy and precision simulated in this paper are most likely smaller than these experimental 1% values. In the simulations of this paper we show that the choice of the ±80% variation indeed results in the correct order of magnitude for the intrinsic accuracy and precision. Another reason for choosing the same 80% variation in this paper, is that there are already published "references values" for the accuracy and precision in Bailey [5]; these values can be used for comparison purposes.

4. The kinetic parameters for levels 10 and 11 in the model

There exist in the literature two sets of experimentally determined kinetic parameters E, s for levels 10 and 11 in the model. The kinetic parameters for TT-OSL signals in quartz were first reported by Li and Li [17], based on direct measurement of isothermal decay of the TT-OSL signals. These authors pointed out the existence of two source traps of the TT-OSL signal and gave an estimation of the related kinetic parameters. The second available set of experimentally determined TT-OSL kinetic parameters are those of Adamiec et al. [2], who used indirect measurement of the TL signals related to the source of TT-OSL. We carried out an initial set of simulations using both sets of parameters, and the results indicated that it is not possible to carry out the ReSAR simulations successfully using the parameters of Li and Li [17]. Examination of the simulated TT-OSL signals obtained using these parameters showed that the temperatures used in the ReSAR protocols were not high enough to thermally transfer a significant amount of charge from these rather deep traps.

We can use the values E, s of the kinetic parameters reported by [17,18]) to estimate the temperature T_{max} of the corresponding putative TL peaks. The value of T_{max} is found from the well known expression [10]:

$$\frac{\beta E}{kT_{max}^2} = s\exp(-\frac{E}{kT_{max}}), \quad (1)$$

where E, s are the kinetic parameters of the trap, β is the heating rate, T_{max} is the temperature corresponding to the maximum TL intensity, and k is the Boltzmann constant. Li and Li [17] reported the following values; $E_1 = 1.14$ eV $s_1 = 1.62 \times 10^6$ s^{-1} for the less thermally stable trap, and $E_2 = 1.55$ eV; $s_1 = 2.5 \times 10^7$ s^{-1} for the deeper and more thermally stable one. These values substituted into Eq. (1) with a heating rate of $\beta = 1$ K/s yield the maximum temperatures at ~480 and 540 °C correspondingly. These temperatures correspond to very deep traps, compared with any of the traps described in the current model. Although these traps certainly would contribute to the TT-OSL signal, we estimate that their contribution is much smaller than the TT-OSL signals originating from shallower traps already existing in the model. On the basis of these simulated results, we decided to carry out *all* the simulations in the paper using the set of kinetic parameters obtained by Adamiec et al. [2]. These values are $E_{10} = 1.46$ eV, $s_{10} = 7.6 \times 10^{11}$ s^{-1}, $E_{11} = 1.72$ eV, $s_{11} = 2.9 \times 10^{12}$ s^{-1} and thermal quenching parameter $W = 0.52$ eV, and are shown in bold in Table 1. The values of all other parameters in Table 1 are those of Pagonis et al. [22,23].

It is noted that our choice of the Adamiec et al. [2] parameters does not mean that the TT-OSL traps studied by Li and Li are not important in TT-OSL processes. Rather, within the limitations of our model, the contribution from these traps to the overall TT-OSL signal is estimated to be small. Ideally, one should include two additional traps to the model which would describe the very deep TT-OSL traps of Li and Li [17]. However, this is beyond the scope of the present simulation study and is expected to be included in future simulation attempts.

5. Simulation of the original ReSAR TT-OSL protocol

We begin by simulating the original single aliquot ReSAR TT-OSL protocol by Wang et al. [35] using the model in Fig. 1, and with the set of parameters shown in Table 1. The detailed steps in the simulation are shown in Table 2 and a typical result of the ReSAR protocol is shown in Fig. 2a. In the example shown we assume that the quartz sample has received a burial dose of 100 Gy in nature, with a dose rate of 3×10^{-11} Gy/s. A sequence of regenerative doses of 0, 80, 100, 120, 80 and 0 Gy is used in the simulated ReSAR protocol. In the example of Fig. 2a, the simulated ReSAR protocol recovers a dose D = 106 Gy, the recycling ratio is 1.05 and the zero dose intensity value is 0.0007. It is clear from this example that the simulation overestimates the burial dose of 100 Gy. This overestimation of the burial dose in the simulation when using the original ReSAR protocol in Table 2 was observed for the majority of the 100 simulated variants. Clearly the parameters in the simulation of the original ReSAR protocol in Table 2 must be adjusted, so that the simulation can reproduce the burial dose with an acceptable precision and accuracy.

We investigated the sources of this inaccurate estimation of the burial dose within the simulated ReSAR protocol, by examining the effect of various parameters on the results of the model. Specifically the simulation of Fig. 2a was repeated by changing a wide variety of parameters in the protocol of Table 2, namely the magnitude of the test dose, the preheat temperature used, and the effect of the additional step 21 in Table 2.

It was found that two experimentally controlled parameters had the biggest effect on the result of the simulation. The most important factor in obtaining good simulated accuracy and precision was found to be the presence of an additional high temperature optical bleaching step between ReSAR/SAR cycles for different regenerative doses. This is listed as step 21 in Table 2.

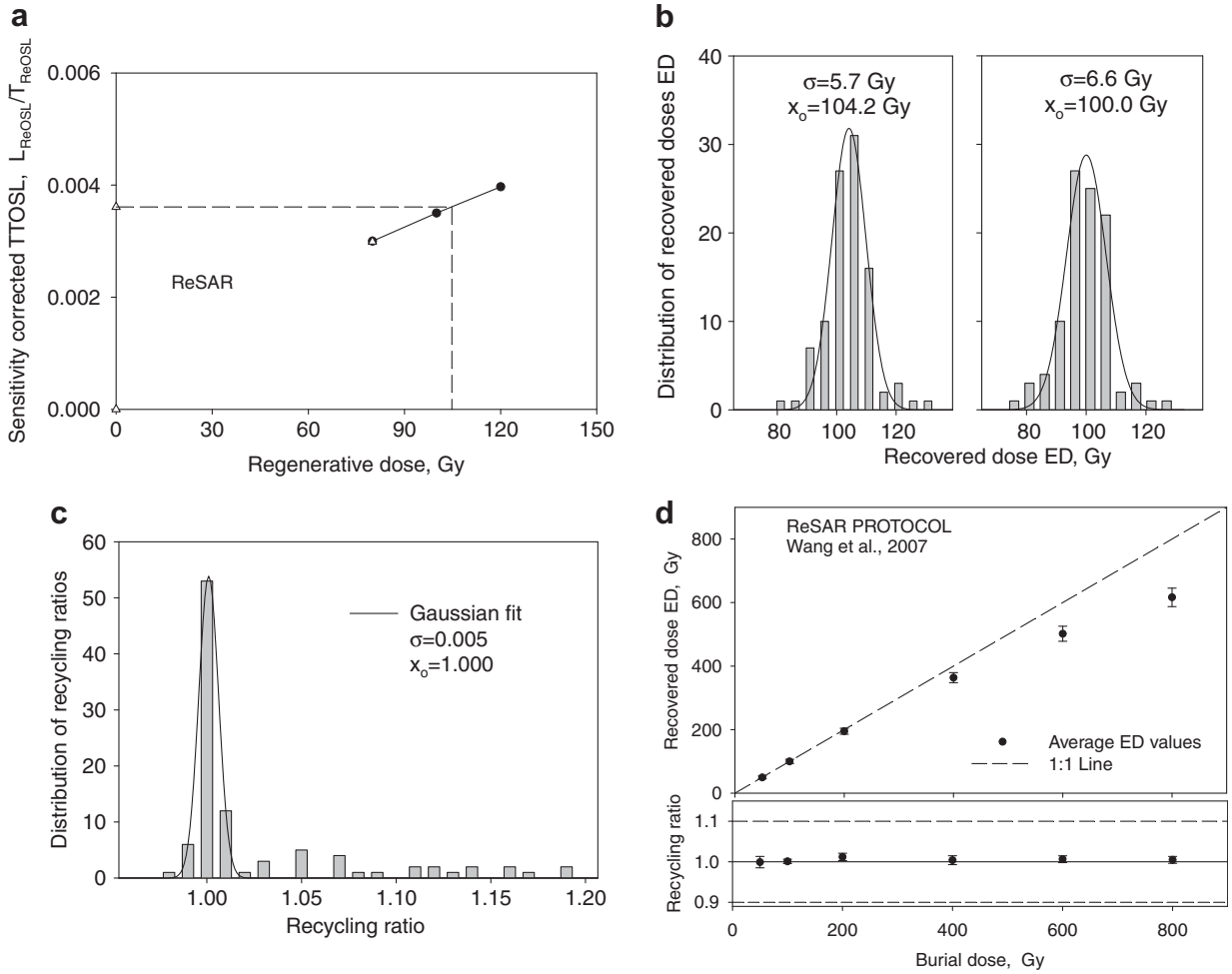

Fig. 2. The results of simulating the ReSAR protocol in Table 2 using the values of the kinetic parameters shown in Table 1. The burial dose D for the natural sample was 100 Gy. The simulation shown in (a) is repeated for $N = 100$ variants of the natural quartz samples as explained in the text. Two histograms are shown, for the original and for the "optimized" parameters in the ReSAR protocol, as described in the text. The resulting distribution of ED values for the "optimized" parameters is fitted to a Gaussian distribution with an average value of 100.0 Gy and a standard deviation of the data given by $\sigma = 6.6$ Gy. The resulting distribution of recycling ratios for the $N = 100$ variants in the model. The ED values obtained from the simulated ReSAR protocol as a function of the burial dose used in the model. The error bars correspond to the standard deviation σ of the 100 model variants, and are calculated with the procedure shown in Fig. 2b; these error bars can be seen to be in the range of 0.5–1% for burial doses up to 200 Gy, and larger for increasing doses. Also shown is the 1:1 line which corresponds to 100% recovery of the burial dose within the model.

The inclusion of this type of step at the end of each cycle has been shown to improve the recovery of the simulated burial dose, as well as the recycling ratio in the protocols. A second factor that has a smaller but significant effect on the accuracy and precision of the simulated ReSAR protocol, was the magnitude of the test dose used for sensitivity corrections.

Fig. 2b and c show the results of our "optimization" of the parameters in the ReSAR simulations, by including a heating step at the end of each cycle in the ReSAR protocol. This heating step consists of heating the sample from room temperature up to 310 °C, as in the course of measuring a TL glow curve. Two histograms are shown in Fig. 2b, for the original and for the "optimized" parameters in the ReSAR protocol.

In order to simulate the *precision* of the optimized ReSAR protocol we have repeated the simulation steps in Fig. 2a using the 100 variants of the natural sample discussed in a previous section. The resulting Gaussian distribution of recovered ED values obtained from the simulations for a burial dose of 100 Gy is shown in Fig. 2b. This distribution of ED values was fitted using a Gaussian function $N(ED)$ of the form:

$$N(ED) = A\exp\left(-\frac{(ED - x_0)^2}{2\sigma^2}\right), \quad (2)$$

where the constant A represents the number of variants at the peak of the distribution which is centered at x_0, and has a standard deviation of the data represented by σ. The fitted Gaussian distribution shown in Fig. 2b is centered at an average value of x_0 = 100.0 Gy (an accuracy of 100% for the expected value of ED = 100 Gy), and has a standard deviation of the data σ = 6.6 Gy corresponding to a precision of the data given by σx_0 = 6.6%. The *standard deviation of the mean* value x_0 will be given by $\sigma_{\text{mean}} = \frac{\sigma}{\sqrt{N}}$ where N = number of data points. In our case N = 100 and we obtain $\sigma_{\text{mean}} = \frac{\sigma}{\sqrt{N}} \sim 0.07$ Gy Our final calculated average ED value for the example in Fig. 2b is reported as ED = (100.00 ± 0.07) Gy.

Fig. 2c shows the corresponding recycling ratios evaluated using the 100 variants. It can be seen that this distribution of recycling ratios is very tightly located around a perfect average recycling ratio of 1.0, with a standard deviation of the data given by σ = 0.005. However, out of the 100 variants simulated in Fig. 2c there are 12 variants which have recycling ratios larger than 1.10. In an experimental situation these cases would have to be rejected as representing inaccurate experimental data. We have identified the source of the large recycling ratios exhibited by these 12 "aliquots"; these large recycling ratios are very closely correlated with parameters very significantly deviated from the "central" values of Table 1. Specifically large recycling ratios correlate with very low values of the concentration of recombination centers in the 12 variants, i.e. with parameter N8 in Table 1. When the value of the total concentration of recombination centers N8 is near the lowest limit of the possible random variations (−80% of the value of N8 in Table 1), the "aliquot" yields recycling ratios larger than 1.10. Nevertheless, Fig. 2b and c show excellent simulated dose recovery and recycling ratio.

The simulation in Fig. 2b and c was repeated for several burial doses between 50 and 800 Gy, and the results are shown in Fig. 2d, which shows the recovered ReSAR equivalent dose ED plotted as a function of the burial dose. The error bars in Fig. 2d correspond to the standard deviation σ of the 100 model variants, and are calculated with the procedure shown in Fig. 2b; these error bars can be seen to be very small for burial doses up to ~200 Gy, and they are in the range of 0.5–1%. We estimate that this value of ~0.1–1% also represents the overall numerical accuracy of the simulations in this paper, due to such factors as numerical approximations during the numerical integration routines in the computer code.

Also shown in Fig. 2d is the 1:1 line which corresponds to 100% recovery of the burial dose within the model. For burial doses D > 400 Gy the ReSAR protocol results in Fig. 2d clearly underestimate the burial dose, with the magnitude of the underestimation becoming larger as the burial dose is increased. This underestimation for burial doses larger than 400 Gy could not be overcome within the model by further optimization of the simulation parameters. The sources of this underestimation are discussed later in this paper, in connection with the thermal stability of the TT-OSL traps in the model.

It must be emphasized that the simulated intrinsic accuracy and precision of the protocols shown in this paper are only one factor influencing the experimentally observed accuracy and precisions of the ReSAR protocols. The overall observed accuracy and precisions will have contributions from several other factors, which are beyond the subject of this paper. The reader is referred to the extensive discussion in the paper by Duller [12] for a more detailed discussion of possible contributions to the accuracy and precision of the SAR-OSL protocol. The interested reader can also find more relevant information on simulated accuracy and precision of the SAR-OSL protocol in the following papers and references therein: [20,11,5,6,12,22,23,25,27,31].

6. Simulation of the SAR-OSL protocol

The simulated data for the ReSAR protocol presented in the previous section were compared with similar simulations carried out using the original and very successful SAR-OSL protocol. This dating protocol was developed during the past 10 years and is known for both high accuracy and precision (see for example [36]. The detailed steps in the protocol are shown in Table 3. We have attempted to optimize the simulated SAR protocol, in a similar manner to the optimized ReSAR protocol in the previous section. We investigated the effect of various parameters in Table 3, namely preheat temperature, magnitude of test dose, cutheat temperature, and inclusion of a high temperature bleaching step between cycles. Once more, inclusion of an additional heating step to 310 °C between cycles was found to be the most important factor influencing the simulated accuracy and precision of the SAR protocol.

The results of our optimized SAR protocol is shown in Fig. 3. Fig. 3a shows a typical example of simulating the SAR-OSL protocol and for a burial dose of 100 Gy. The five regenerative doses used in the example of Fig. 3a were 0, 80, 100, 120, 0 and 80 Gy, and the test dose used was 5 Gy. The preheat temperature used in the SAR protocol simulation was 10 s at 260 °C for the regenerative dose measurements, and the cut-heat used for the test dose measurements was 20 s at 220 °C. The sensitivity corrected signals L/T shown in Fig. 3a were used to reconstruct the dose response curve, and as usual interpolation was used for estimating the equivalent dose ED by the sample. In the example shown in Fig. 3a, the recycling ratio was 1.04, the zero-dose intensity was 0.14 and the recovered dose was ED = 99.1 Gy.

The result of simulating 100 variants within the SAR-OSL technique for a burial dose D = 100 Gy is shown in Fig. 3b, and is fitted with a Gaussian distribution function shown as a solid line. The resulting Gaussian distribution of the ED values has a standard deviation of the data given by σ. The fitted Gaussian distribution for the SAR-OSL technique in Fig. 3b is centered at x_0 = 101.5 Gy and the standard deviation of the data is σ = 4 Gy. In the example of Fig. 3b we did not obtain 100% recovery of the average dose in the SAR simulations. It is likely that by further optimization of the parameters in the SAR simulation one can obtain 100% dose recovery, although as discussed above, numerical approximations made during numerical integrations are likely a limiting factor estimated to be of the order of 0.1–1%. We therefore consider the

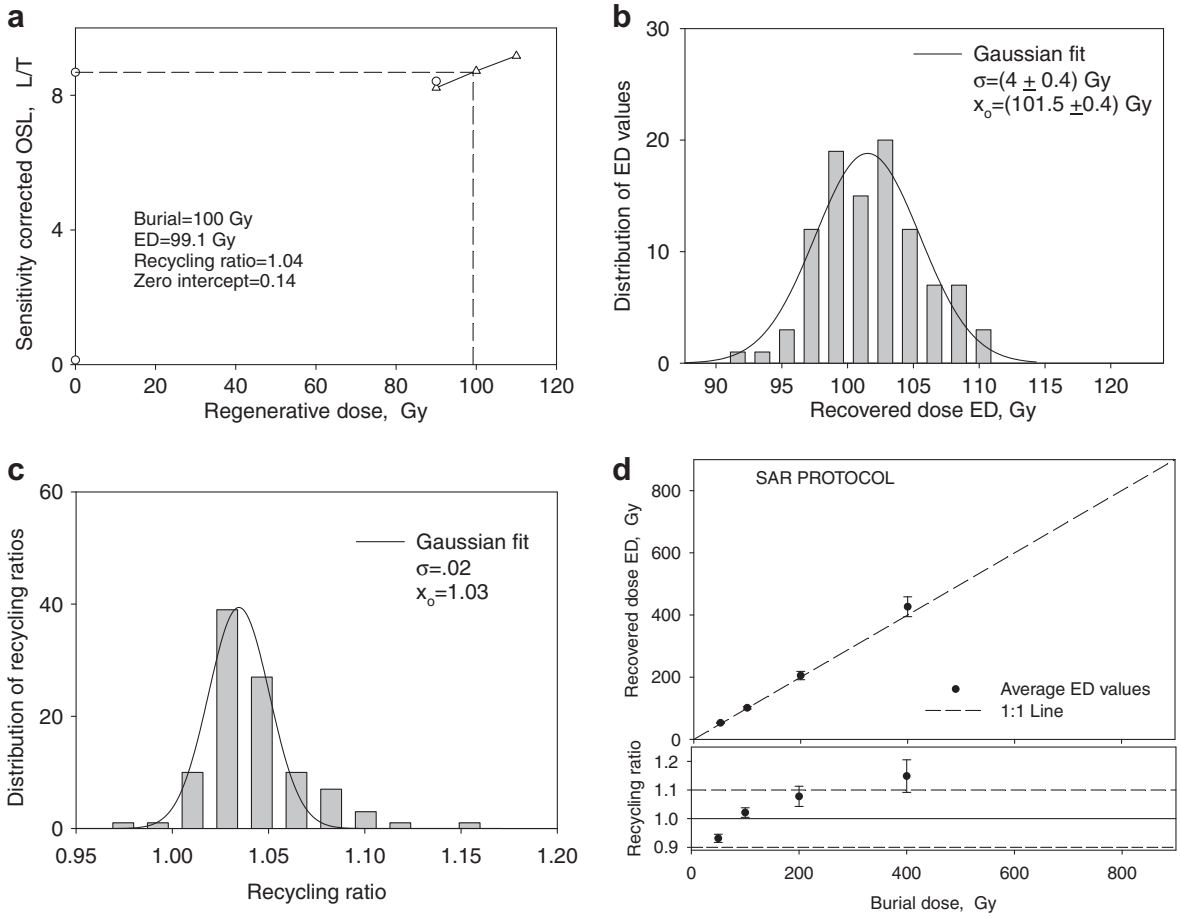

Fig. 3. The results of simulating the SAR-OSL protocol in Table 3 using the values of the kinetic parameters shown in Table 1. The burial dose D for the natural sample was 100 Gy. The simulation shown in (a) is repeated for $N = 100$ variants of the natural quartz samples as explained in the text. The resulting distribution of ED values is fitted to a Gaussian distribution with an average value of 101.5 Gy and a standard deviation of 4 Gy. The resulting distribution of recycling ratios for the $N = 100$ variants in the model, for the SAR protocol. The ED values obtained from the simulated SAR-OSL protocol are plotted as a function of the burial dose D used in the model. The error bars correspond to the standard deviation σ of the 100 model variants, and are calculated with the procedure shown in Fig. 3b. Also shown is the 1:1 line which corresponds to 100% recovery of the burial dose within the model.

dose recovery averages shown in Figs. 2c and 3c as indicating successful recovery of the burial doses and good recycling ratios, within both the SAR and ReSAR protocols.

The ratio $\sigma/x_0 = 4/101.5 = 0.04 = 4\%$ provides an estimate of the intrinsic precision of the SAR-OSL protocol at the burial dose of $D = 100$ Gy. The corresponding distribution of 100 recycling ratios is shown in Fig. 3c. The Gaussian fit to this distribution yields an average recycling ratio of 1.03 with a standard deviation of the data given by 0.02. It is noted that the distribution shown for the SAR protocol in Fig. 3c is significantly wider than the corresponding distribution for the ReSAR protocol in Fig. 2c.

Fig. 3d shows the results of the SAR-OSL simulation for burial doses in the range 0–400 Gy. The error bars shown in Fig. 3d correspond to the standard deviation σ of the 100 model variants, and represent the standard deviation of the 100 ED values obtained at each dose. The value of σ provides an estimate of the simulated *intrinsic precision* of the SAR-OSL protocol at the various doses. As can be seen in Fig. 3d, the simulated precision gets increasingly worse at higher doses. The corresponding average recycling ratios at each burial dose are shown at the bottom of Fig. 3d, and they are also seen to increase systematically at higher doses, and they also become larger than the accepted limit of 1.1 in the same dose region. We attribute the overestimation of these higher doses during the SAR protocol to this incomplete recycling.

We conclude that Fig. 3d shows that the simulated SAR-OSL technique can reproduce doses in the complete dose region up to at least 200 Gy with an accuracy of ~1%. The OSL and TT-OSL dose response curves are simulated and discussed in the next section.

7. Simulations of the OSL dose response of the quartz samples

We carried out a simulation of the OSL dose response of the quartz sample by using the same model and same set of kinetic parameters from Table 1. A series of regenerative doses $D_i = 0$, 10, 20, 50, 100, 200, 400 Gy are given to the natural sample and the SAR-OSL protocol is used to obtain the sensitivity corrected OSL signals L/T. These simulations of the OSL dose response were repeated using the 100 variants of the natural quartz sample, and the resulting dose response curves were averaged. The result of averaging these 100 dose response curves are shown in Fig. 4a for the SAR-OSL protocol. The error bars shown in Fig. 4a correspond to the standard deviation $\sigma_{mean} = \sigma/\sqrt{N}$ of the average $(L/T)_{average}$ values, where σ represents the standard deviation of the $N = 100$ L/T values obtained at each dose. The value of σ_{mean} in this case provides an estimate of the intrinsic precision of the L/T measurements at the various doses. As can be seen in Fig. 4a, the simulated precision σ_{mean} gets increasingly worse at higher doses. In addition to the average growth curve, two additional growth curves are shown in Fig. 4a corresponding to the 95% confidence limits of the average L/T values. These additional growth

curves provide an estimate for the range of variation of growth curve shapes that can result from changing the parameters in the model.

A typical example of the distribution of the sensitivity corrected L/T signals at a dose of 200 Gy are shown in the form of a histogram in Fig. 4b. The resulting Gaussian distributions of the L/T values were fitted once more with a Gaussian distribution, with the standard deviation of the L/T data given by σ. The fitted Gaussian distribution for the SAR-OSL technique in Fig. 3b is centered at a mean value $x_0 = (L/T)_{average} = 14.2$ a.u. and the standard deviation of the data is $\sigma = 3.65$ a.u. The ratio $\sigma/x_0 = 0.25$ provides an estimate of the precision of the L/T measurements at a dose $D = 200$ Gy.

8. Simulations of the TT-OSL ReSAR dose response of the quartz samples

The simulations of the dose response curves shown in Fig. 4 were repeated using the original ReSAR protocol of Wang et al. [35] and with our optimized ReSAR protocol. As in the previous section, a simulated series of regenerative doses D_i = 0, 10, 20, 50, 100, 200, 400, 800, 1600 Gy are given to the natural sample and the ReSAR protocol is used to obtain the sensitivity corrected TT-OSL signals L_{ReOSL}/T_{ReOSL} at the different doses. The simulation is then repeated for the 100 natural variants of the sample. The resulting average dose response curve for the ReSAR protocol is shown in Fig. 5a, and a typical distribution of the L/T values for the 100 sample variants at a regenerative dose $D = 400$ Gy is shown in Fig. 5b. The error bars in Fig. 5a correspond to the standard deviation $\sigma_{mean} = \sigma/\sqrt{N}$ of the average L/T values, and can be seen that they are in the range of 1–10%. In addition to the average growth curve, two additional growth curves are shown corresponding to the 95% confidence limits of the average L/T values. The corresponding growth curve of the OSL signal from Fig. 4a is also shown, for comparison purposes.

Inspection of Fig. 5a and comparison with Fig. 4a shows that the L/T dose response curve for the thermally transferred ReSAR signal continuously increases almost linearly even at very high doses of 800 Gy. It is noted that the corresponding OSL signal in Fig. 4a also has not reached saturation even at doses of 800 Gy. This is consistent with the experimental results of Wang et al. [35] and also with previous simulations of the ReSAR protocol by Pagonis et al.

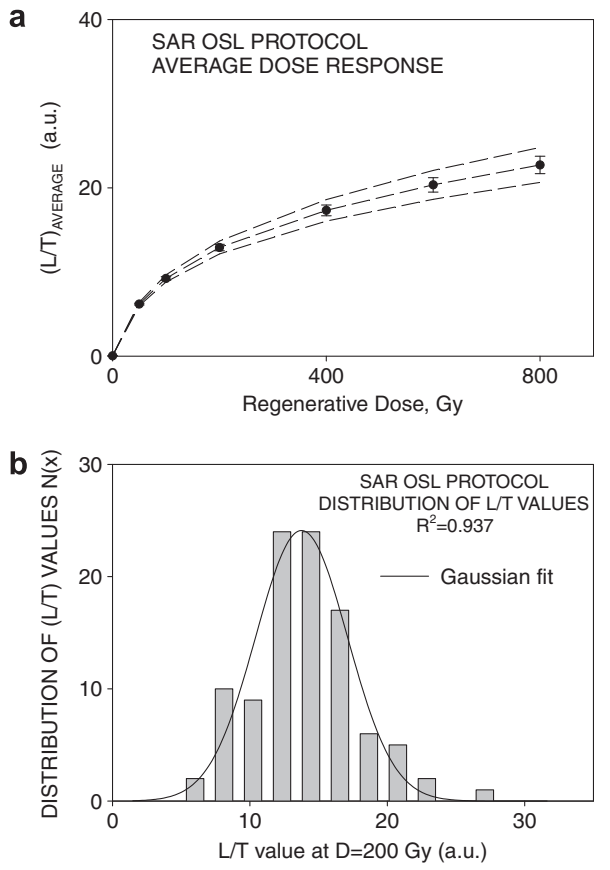

Fig. 4. (a) The result of averaging 100 dose response curves obtained by simulating the SAR-OSL protocol for the 100 natural sample variants. The error bars shown correspond to the standard deviation of the mean L/T values $\sigma_{mean} = \sigma/\sqrt{N}$, where σ represents the standard deviation of the 100 L/T values obtained at each dose. The value of σ_{mean} in this case provides an estimate of the intrinsic precision of the L/T measurements at the various doses. The simulated precision σ_{mean} gets increasingly worse at higher doses. In addition to the average growth curve, two additional growth curves are shown corresponding to the 95% confidence limits of the average L/T values. (b) A typical example of the distribution of the sensitivity corrected L/T signals at a dose of 200 Gy are shown in the form of a histogram. The resulting distribution of the 100 L/T values were fitted with a Gaussian distribution centered at a mean value $x_0 = (L/T)_{average} = 14.2$ a.u. and the standard deviation of the data is $\sigma = 3.65$ a.u.

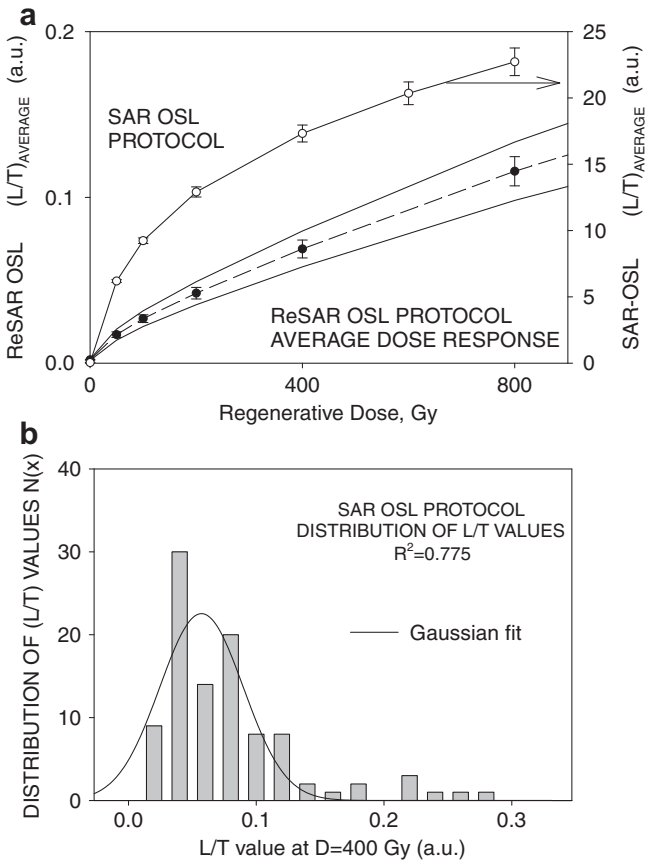

Fig. 5. (a) The result of averaging 100 dose response curves obtained by simulating the ReSAR protocol of Wang et al. [35] using 100 natural sample variants. The error bars shown correspond to the standard deviation of the mean ED values $\sigma_{mean} = \sigma/\sqrt{N}$, where σ represents the standard deviation of the 100 ED values obtained at each dose. The value of σ_{mean} in this case provides an estimate of the intrinsic precision of the ReSAR protocol at the various doses. The simulated precision σ_{mean} gets increasingly worse at higher doses. In addition to the average growth curve, two additional growth curves are shown, corresponding to the 95% confidence limits of the average L/T values. The corresponding growth curve of the OSL signal from Fig. 4a is also shown, for comparison purposes. (b) A typical example of the distribution of the sensitivity corrected L/T signals at a dose of 400 Gy are shown in the form of a histogram. The resulting distribution of the 100 ED values were fitted with a Gaussian distribution.

[22,23] (see their Fig. 3 showing a direct comparison of modeled and experimental dose response curves).

9. Simulations of sensitivity changes occurring during successive irradiations with the same dose

Wintle and Murray [36] suggested carrying out tests of sensitivity changes occurring during the SAR-OSL protocol, by carrying out successive cycles of sample irradiation with the same dose D, followed by a measurement of the sensitivity corrected OSL L/T signal. In such sensitivity tests one plots the test dose OSL signal (termed the T-signal) as a function of the corresponding uncorrected OSL signal (termed the L-signal). Such graphs of L vs. T should be linear and should pass through the origin of the graph. During the past few years several authors have published such experimental L–T graphs for both the SAR-OSL and ReSAR TT-OSL protocols, but there has been no systematic simulation study of this type of measurement. Furthermore, there are no published simulations of L–T graphs for the ReSAR protocol in the literature. In this section we describe such L–T simulations for the SAR-OSL and ReSAR protocols; our goal is to examine what experimental factors could be affecting the L–T graphs, and to carry out a comparison of these types of graphs between the two protocols.

Typical results of simulating the L–T experiments are shown in Fig. 6a for the SAR-OSL protocol, and in Fig. 6b and c for the ReSAR protocol. Fig. 6a shows the results of the sensitivity test for the SAR protocol consisting of 10 cycles of a regenerative dose $D = 20$ Gy, using the parameters in Table 1. The natural dose of the simulations in Fig. 6a–c is 1 Gy, and the test dose used in both the SAR and ReSAR protocol examples of Fig. 6 is 7 Gy. The L–T graph is seen to be linear and passing close to the origin. These simulated results are similar to the experimental TT-OSL data shown by Wang et al. [35], their Fig. 2.

Fig. 6b and c show an example of simulating the sensitivity test for the more complex ReSAR protocol, consisting of 10 cycles of a regenerative dose $D = 1000$ Gy, using the parameters in Table 1 and a test dose TD = 7 Gy. During this sensitivity test one obtains the L–T graphs for the TT-OSL signal, as well as corresponding L–T graphs for the less optically sensitive basic-TT-OSL (B-TT-OSL) signal. These two simulated L–T graphs are shown in Fig. 6b and c. It is seen that both L–T graphs are linear and pass close to (but not exactly through) the origin.

These simulations of the L–T graphs were repeated using several different test doses in the ReSAR protocol, in order to examine the effect of the test dose (TD) on the L–T graphs. The results of these simulations for different test doses are shown in Fig. 7a and b. The regeneration doses in Fig. Fig. 7a and b are 1000 Gy. Fig. 7a shows the L–T graphs when using test doses with values TD = 0.1, 7 and 100 Gy. Fig. 7b shows the same data as Fig. 7a, normalized to the first L–T measurement; the normalized data shows clearly that higher test doses result in larger y-intercepts in the L–T graphs. The important observation here is that the simulated linear data in Figs. 6b and 7a show a positive intercept with the T-axis. This type of behavior for the T-intercept has been reported by Athanassas and Zacharias [3], their Fig. 6. However, the experimental data of Tsukamoto et al. [32] show a *negative* T-intercept instead (see their Fig. 3). These results show that different types of quartz samples can exhibit either a positive or a negative T-intercept during this type of sensitivity change experiment.

It is noted that even though the L–T lines in Fig. 6b and c do not pass through the origin, the accuracy and precision of the ReSAR protocol at the regenerative dose of $D = 1000$ Gy does not seem to be affected. This is in agreement with several reported experimental L–T graphs, in which the ReSAR protocol was applied successfully, even though the L–T graphs do not seem to pass exactly through the origin, or may even not be perfect straight lines [32,30,26,15]. The simulated results in Fig. 7 demonstrate that the magnitude of the test dose can have a large effect on the observed sensitivity changes during the ReSAR protocol.

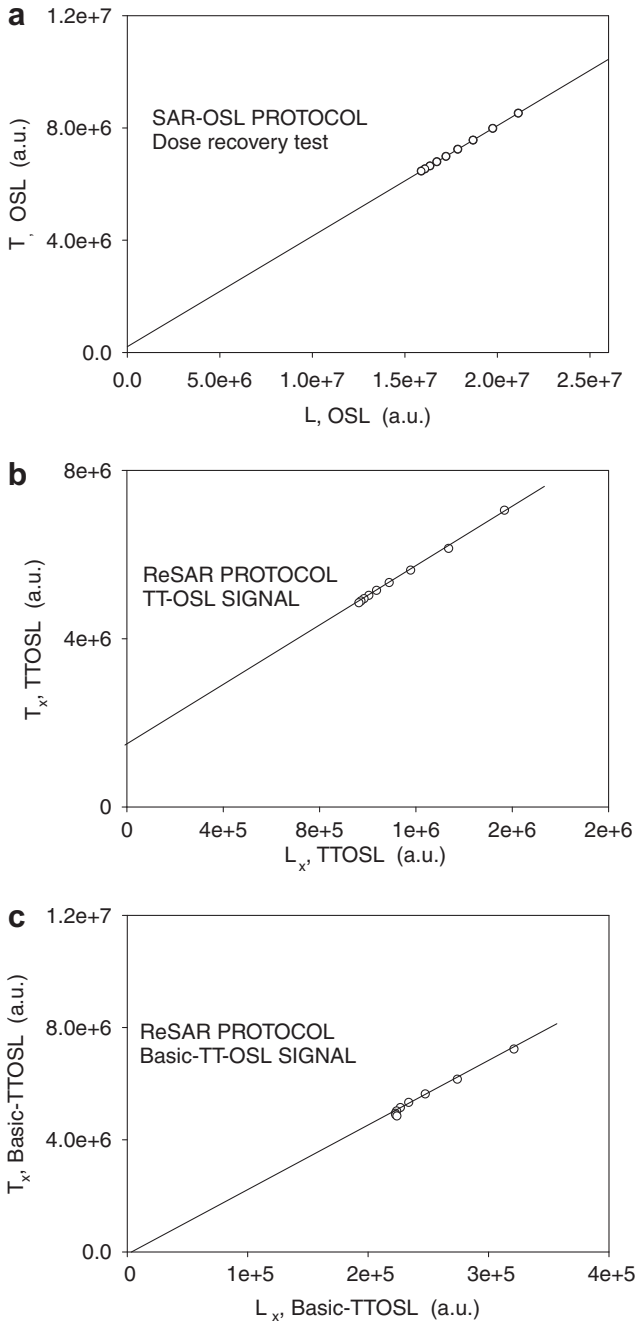

Fig. 6. (a) Simulations of the sensitivity test (L–T graphs) suggested by Wintle and Murray [36], consisting of successive cycles of sample irradiation with the same dose D, followed by measurement of the sensitivity corrected SAR-OSL L/T signal. Such graphs of L vs T should be linear and should pass through the origin of the graph. The results shown are for the SAR-OSL protocol and for 10 cycles of a regenerative dose $D = 20$ Gy, using the parameters in Table 1. The L–T graph is linear and passes very close to the origin. (b) An example of simulating the L-T sensitivity test for the more complex ReSAR protocol. Here 10 cycles of a regenerative dose $D = 1000$ Gy are simulated using the parameters in Table 1 and a test dose TD = 7 Gy. The burial dose was 1 Gy. The results shown are for the ReOSL part of the TT-OSL signal. (c) Simulated L–T graphs for the second component of the TT-OSL signal, the less optically sensitive basic-TT-OSL (B-TT-OSL) signal. The two simulated L–T graphs in (b) and (c) are linear and pass again close but not exactly through the origin.

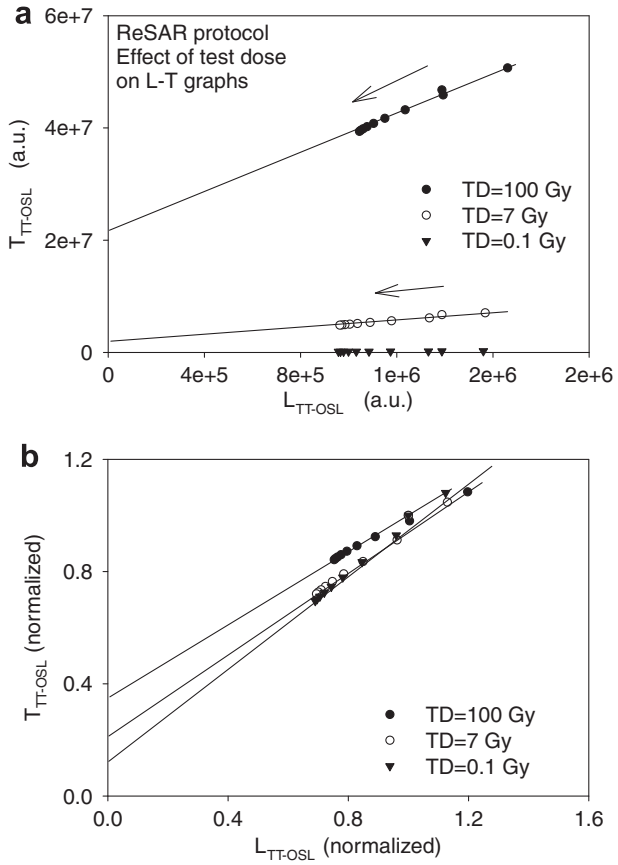

Fig. 7. The effect of the test dose (TD) on the L–T graphs for the ReSAR protocol. (a) The simulated L–T graphs when using test doses with values TD = 0.1, 7 and 100 Gy. (b) Shows the same data as (a) normalized to the first L–T measurement; the normalized data shows clearly that higher test doses result in larger y-intercepts in the L–T graphs.

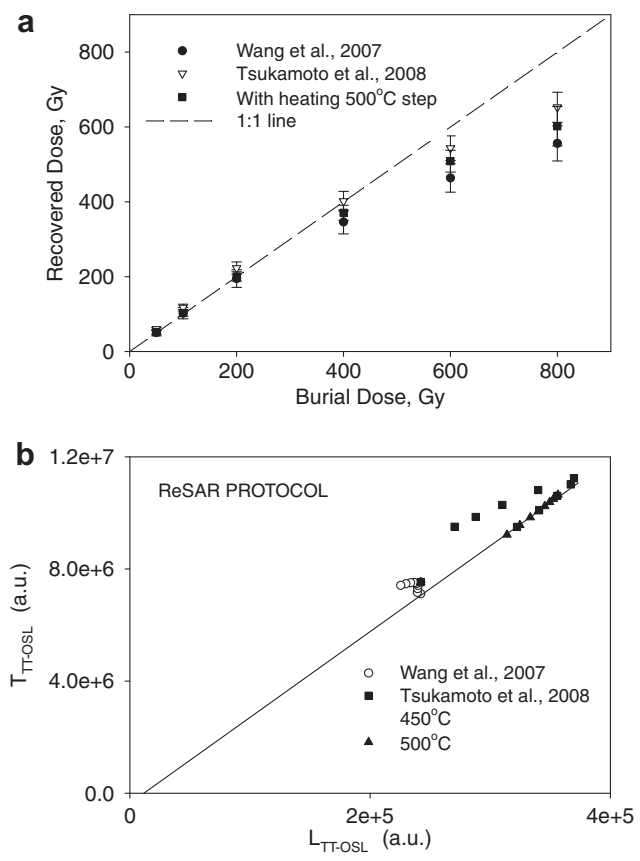

Fig. 8. (a) Simulations of the modified ReSAR protocol of Tsukamoto et al. [32]. An extra step in added in the protocol of Table 2, consisting of a high temperature optical bleaching between regeneration cycles (triangles). The solid circles show the effect of a heating step at 500 °C. (b) Simulations of the effect of the extra step on the L–T graphs obtained using successive 1000 Gy irradiations. The natural sample here had received a burial dose of 1 Gy, and was optically bleached in the laboratory. The test dose used was 0.1 Gy. These results show that adding the high temperature optical bleaching affects the shape of the L–T graphs in a rather dramatic fashion. When the original ReSAR protocol is used (circles) one observes very small changes in the sensitivity between cycles, and the points in the graph are crowded together around the same L and T values. When a high temperature optical bleaching is added in the range of 400–500 °C, the L–T graphs become more linear indicating larger sensitivity changes between successive cycles (solid symbols).

10. Simulations of modified ReSAR protocols suggested by various researchers

Several authors have developed and tested several modified and/or simplified versions of the ReSAR protocol, which can result in very significant time savings during dating of samples using the TT-OSL signals. In this section we present simulations for several of these alternative proposed ReSAR protocols, and compare their relative accuracy and precisions at a wide range of burial doses.

Tsukamoto et al. [32] in a comprehensive study of the TT-OSL ReSAR protocol, tested various versions of the original protocol by Wang et al. [35]. These authors suggested several modifications which may improve the accuracy of the ReSAR protocol. Furthermore, they studied the temperature dependence, dose response and bleaching characteristics of TT-OSL signals from several quartz loess samples from China and from coastal sands in South Africa. They suggested a modified protocol in which a step is added consisting of blue light stimulation for 100 s at 280 °C at the end of each ReSAR cycle. By adding this high temperature bleach step and by using a component separation of ReOSL signal, it was found that the ReSAR protocol could recover given doses up to at least 1000 Gy.

Fig. 8a shows the results of simulating the modified ReSAR protocol of Tsukamoto et al. [32], by adding a high temperature optical bleaching step to the original ReSAR protocol suggested by Wang et al. [35]. This extra step is shown as Step 21 in Table 2. The simulated results of Fig. 8a show that both the original and the modified ReSAR protocols can reproduce the natural doses accurately up to at least 400 Gy, and that burial doses above 400 Gy tend to be systematically underestimated. In Fig. 8b we show the effect of adding an extra *heating* step at the end of the protocol by Wang et al. [35], as suggested by Tsukamoto et al. [32]. Two examples are shown in Fig. 8b, with the heating step consisting of heating the sample for 100 s at 450 and 500 °C. The simulated L–T graphs shown are obtained using successive 1000 Gy irradiations and L–T measurements.

The simulations in Fig. 8b show that adding the high temperature optical bleaching affects the L–T graphs in a rather dramatic fashion. When the original ReSAR protocol is used (open circles) one observes very small changes in the sensitivity between cycles, and the points in the graph are crowded together around the same L and T values. The natural sample here had received a burial dose of 1 Gy, and was optically bleached in the laboratory, while the test dose used was 0.1 Gy. When a high temperature heating step is added at the end of the ReSAR protocol, the L–T graphs become more linear indicating larger sensitivity changes between successive cycles. The simulated data in Fig. 8b are similar but not identical to published L–T graphs by several researchers [32,30,3].

Several researchers have very recently suggested simplified versions of the original ReSAR protocol by Wang et al. [26,30,2,3]. The simplified protocol suggested by Porat et al. [26] is listed in Table 4,

and the simulated results for this protocol are shown in Fig. 9. Fig. 9a shows a typical example of the distribution of ED values obtained by simulating the Porat et al. protocol for a burial dose of D = 200 Gy. Fig. 9b shows that this simplified version of the ReSAR protocol reproduce accurately doses up to ~400 Gy, while it clearly underestimates doses above 400 Gy. Also shown in Fig. 9b is the effect of the initial preheat step used in the Porat et al. protocol on the accuracy of the protocol. This preheat step is shown as step 6 in Table 4.

Stevens et al. [30] found difficulties in applying the ReSAR protocol to Chinese loess samples, including poor recycling, non-linear L–T graphs and L–T graphs with negative intercepts. They suggested a modified protocol in which sensitivity changes are monitored by the response of the TT-OSL signal to a test dose, and there is no correction for BT-OSL signals. Their protocol uses high temperature optical bleach in the middle and at the end of each cycle, in order to clear the traps and remove any remaining TT-OSL signal after each regenerative dose. Their simplified protocol was applied successfully to several quartz samples; however, they noted the presence of weak signals as one of the important limiting factors in applying the protocol to many of the studied samples. The simplified protocol suggested by Stevens et al. [30] contains two extra high temperature optical bleaching steps, consisting of CW-OSL optical excitation for 400 s at 290 °C. These steps are shown as numbers 10 and 14 in Table 5. The simulated results for this simplified protocol are shown in Fig. 10.

Finally, in a recently published study Adamiec et al. [2] carried out a series of experiments designed to determine the kinetic parameters of the TT-OSL source traps. These authors studied both the TL and OSL signals measured during typical TT-OSL measurements, and found a correspondence between TL peaks and the TT-OSL signal. By using a variable heating rate method of analysis, the thermal stability of the main TT-OSL trap was studied in detail, and an improved TT-OSL ReSAR protocol was proposed. The simplified protocol suggested by Adamiec et al. [2] is listed in Table 6, and the simulated results for this protocol are shown in Fig. 10.

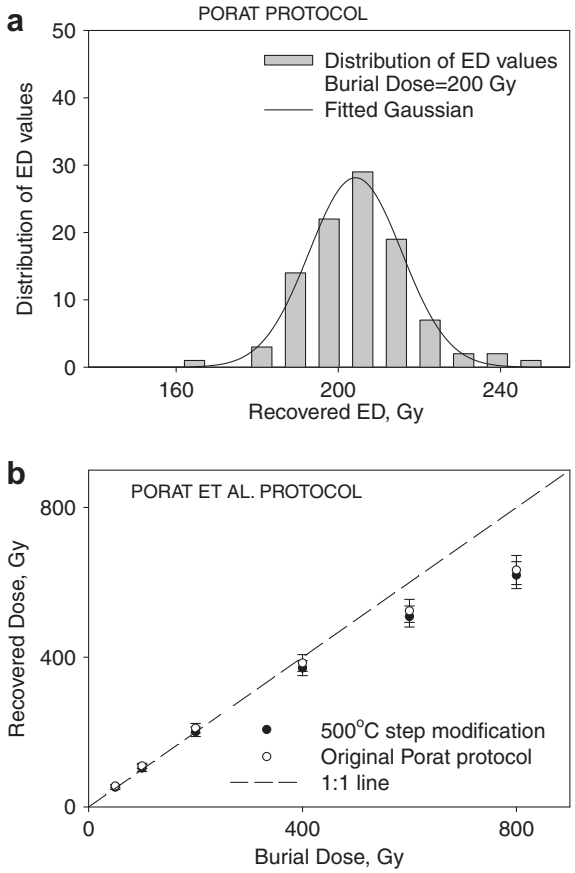

Fig. 9. The results of simulating the simplified ReSAR protocol suggested by Porat et al. [26]. The steps in this protocol are listed in Table 4. (a) A typical example of the distribution of ED values obtained by simulating the Porat et al. protocol for a burial dose of D = 200 Gy. (b) The Porat et al. protocol can reproduce accurately burial doses up to ~500 Gy, while some dose underestimation is evident above 400 Gy.

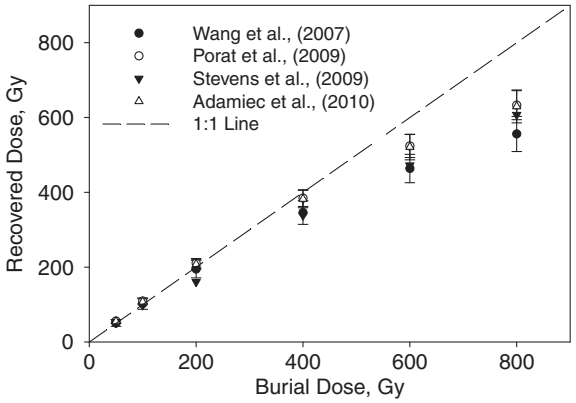

Fig. 10. The results of simulating the simplified ReSAR protocol suggested by Adamiec et al. [2] is compared with those of the Porat et al., Wang et al. and Stevens et al. protocols. The steps in the protocols of Stevens et al. [30] and of Adamiec et al. [2] are listed in Tables 5 and 6.

Fig. 10 compares the simulated intrinsic accuracy and precision of the Adamiec, Porat, Stevens and Wang protocols in the burial dose range 0–800 Gy. The same set of kinetic parameters from Table 1 is used for all 4 protocols in Fig. 10. It can be seen that all 4 versions of the protocol have very similar intrinsic precisions, but their intrinsic accuracy varies at the different burial doses. The simulation results of the previous sections showed that the intrinsic accuracies of these protocols depend on several experimentally controllable conditions (such as the test dose, preheat temperatures and high temperature steps at the end of the protocols).

An important point deduced from Fig. 10, is that all 4 protocols underestimate the equivalent dose delivered in natural conditions at high dose above ~400 Gy. However Adamiec et al. [2] found that *laboratory* doses in excess of 800 Gy could be recovered accurately using their protocol. We have simulated the recovery of a 1000 Gy *laboratory* dose by using the protocol of Adamiec et al. [2], and found that the ED value recovered in the simulation was (1118 ± 101) Gy. This seems to indicate that the difference between the natural and laboratory dose rates may be one of the contributing factors to the underestimation of the burial doses above 400 Gy.

The underestimations at high doses shown in Fig. 10 are not due to possible saturation of the TT-OSL signal at high doses, since the simulated TT-OSL signal is not saturated even at very high doses of 4000 Gy. We have investigated the thermal stability of the TT-OSL source traps as another possible reason for this underestimation within the protocols.

In an attempt to identify a possible source for the underestimations shown in Fig. 10, we have repeated a set of simulations by varying the energy of the TT-OSL source trap (parameter E_{10} for level 10 in the model of Fig. 1). Increasing this energy results in a simulated thermally more stable trap. Specifically we increased the energy value between 1.65 and 1.85 eV, with the simulated results shown in Fig. 11 for a burial dose of 800 Gy in the model. As can be seen in Fig. 11, by increasing the energy of the TT-OSL source trap the protocol reproduces the burial dose more accurately. In other words, by making the source trap more thermally

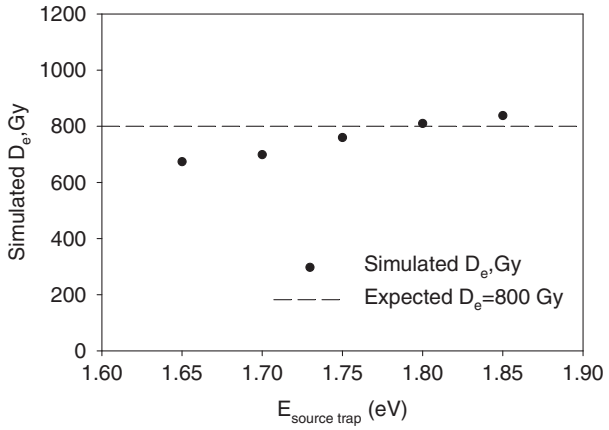

Fig. 11. The results of a set of simulations carried out by varying the energy of the TT-OSL source trap using the model of Fig. 1, and for a burial dose of 800 Gy. Increasing this energy of the source trap results in the protocol reproducing the burial dose more accurately. This suggests that a more thermally stable source trap may result in more accurate determination of equivalent doses within the model.

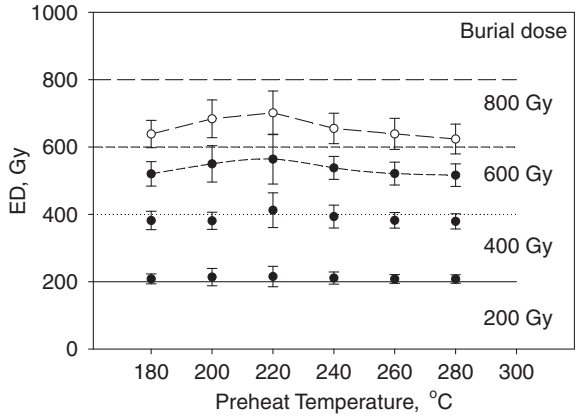

Fig. 12. Simulations the preheat plateaus for natural doses of 200, 400, 600 and 800 Gy. In the case of 200 and 400 Gy the simulated ED doses are constant at all preheat temperatures, and the natural doses are reproduced accurately by the ReSAR protocol. However, for the higher natural doses of 600 Gy and 800 Gy an "optimal" preheat temperature is located at around 220 °C.

stable within the model results in more accurate determination of high equivalent doses.

We conclude that the thermal stability of the TT-OSL trap may be one of the reasons that the simulated protocols underestimate the equivalent doses for burial doses larger than ~400 Gy. Further experimental work and modeling are necessary to establish the exact reason for the simulated underestimates of the equivalent doses shown in Fig. 10. One of the best methods to investigate the effect of thermal stability on dose underestimation is to check the preheat plateau. Fig. 12 shows the results of simulating the preheat plateaus for natural doses of 200, 400, 600 and 800 Gy. In the case of 200 and 400 Gy the simulated ED doses are constant at all preheat temperatures, and the natural doses are reproduced accurately by the ReSAR protocol. However, for the higher natural doses of 600 and 800 Gy, the results of Fig. 12 indicate a non-constant plateau, and that the "optimal" preheat temperature is located at around 220 °C. One must note that even in the case of the "optimal" preheat temperature, the natural doses of 600 and 800 Gy are still significantly underestimated by more than ~10%. Furthermore, the size of the error bars in Fig. 12 shows that the precision of the ReSAR protocol becomes worse at this optimal preheat temperature. On the basis of the simulated results of Fig. 12, we conclude that the simulated underestimation of natural doses larger than 400 Gy must have a rather complex physical origin, which necessitates further study using both simulations and experiment.

Another point to be mentioned here, is that the thermal stability of traps is not only dependent on the energy depth *E*, but also on the frequency factor, *s*. Changing the value of *s* would also result in a change in lifetime, which means that the underestimation seen in the simulation could also be a result of inappropriately choosing the value of *s*.

11. Discussion and conclusions

The kinetic model used in this paper includes only the fast and medium components, while the model does not contain the slow components known to exist in quartz samples. One cannot exclude the possibility that these slow components could make a significant contribution to the process of thermal transfer. Such components have been shown to be more important than the fast and medium components in thermal transfer processes [16,19]. This is certainly a limitation in the current model.

Another limitation has to do with the parameters used here for the medium component (level 4 in the model). Experimental studies have reported that the thermal stability of this component may be sample dependent. Jain et al. [16] and [29] reported that this component may be more stable than the fast component, while Li and Li [18] and [28] reported a less thermally stable component. In the latter case, the medium component results in underestimation in SAR protocol, similar to the underestimation presented in this paper for high doses. Our model uses the kinetic parameters of the medium component from [29], whose sample has a stable medium component. It is then possible that the present model may only apply to quartz samples with a stable medium component. This is a general limitation of all quartz models; one cannot expect all quartz samples to exhibit the same behavior, and this has been shown clearly in several experimental studies.

Ideally, one should include several additional traps to the model which would describe the very deep TT-OSL traps of Li and Li [17], as well as the slow components previously studied by several researchers. This is beyond the scope of this paper, and should be the subject of further experimental and modeling work.

The comprehensive quartz model of Pagonis et al. [22,23] was used successfully in this paper to simulate the complete sequence of experimental steps taken during several recently published versions of the ReSAR dating protocol. The relative intrinsic accuracy and intrinsic precision of these protocols were simulated by analyzing 100 random variants of the natural samples, and by fitting Gaussian probability functions to the resulting distribution of ED values. Several factors which may be affecting both the precision and the accuracy of four different versions of the ReSAR protocols were investigated. New simulations are presented of sensitivity changes occurring during the SAR-OSL and the ReSAR protocols, and the possible shapes of the L–T graphs were found to be in general qualitative agreement with published L–T graphs. The simulations showed that all 4 versions of the protocol have very similar intrinsic precisions; however, their intrinsic accuracy varies at the different burial doses and depends on several experimentally controllable conditions.

Acknowledgements

We thank an anonymous reviewer for their very constructive and insightful comments, which have resulted in a comprehensive revision of this paper.

References

[1] G. Adamiec, R.M. Bailey, X.L. Wang, A.G. Wintle, The mechanism of thermally transferred optically stimulated luminescence in quartz, J. Phys. D Appl. Phys. 41 (2008) 135503.

[2] G. Adamiec, G.A.T. Duller, H.M. Roberts, A.G. Wintle, Improving the TT-OSL SAR protocol through source trap characterization, Radiat. Meas. 45 (2010) 768–777.

[3] C. Athanassas, N. Zacharias, Recuperated-OSL dating of quartz from Aegean (South Greece) raised Pleistocene marine sediments current results, Quat. Geochronol. 5 (2010) 65–75.

[4] R.M. Bailey, Towards a general kinetic model for optically and thermally stimulated luminescence in quartz, Radiat. Meas. 33 (2001) 17–45.

[5] R.M. Bailey, Paper I – simulation of dose absorption in quartz over geological timescales and its implications for the precision and accuracy of optical dating, Radiat. Meas. 38 (2004) 299–310.

[6] R.M. Bailey, S.J. Armitage, S. Stokes, An investigation of pulsed-irradiation regeneration of quartz OSL and its implications for the precision and accuracy of optical dating (Paper II), Radiat. Meas. 39 (2005) (2005) 347–359.

[7] I.K. Bailiff, The pre-dose technique, Radiat. Meas. 23 (1994) 471–479.

[8] I.K. Bailiff, Retrospective dosimetry with ceramics, Radiat. Meas. 27 (1997) 923–941.

[9] J.K. Bailiff, N. Holland, Dating bricks of the last two millennia from Newcastle upon Tyne: a preliminary study, Radiat. Meas. 32 (2000) 615–619.

[10] R. Chen, S.W.S. McKeever, Theory of Thermoluminescence and Related Phenomena, World Scientific Publishing, Singapore, 1997.

[11] G. Chen, A.S. Murray, S.H. Li, Effect of heating on the quartz dose–response curve, Radiat. Meas. 33 (2001) 59–63.

[12] Duller (2007). Assessing the error on equivalent dose estimates derived from single aliquot regenerative dose measurements. Ancient TL, 25, 15–24.

[13] A. Galli, M. Martini, C. Montanari, L. Panzeri, E. Sibilia, TL of fine-grain samples from quartz-rich archaeological ceramics: Dosimetry using the 110 and 210 C TL peaks, Radiat. Meas. 41 (2006) 1009–1014.

[14] H.Y. Göksu, D. Stoneham, I.K. Bailiff, G. Adamiec, A new technique in retrospective TL dosimetry: pre-dose effect in the 230 C TL glow peak of porcelain, Appl. Rad. Isot. 49 (1998) 99–104.

[15] J.C. Kim, G.A.T. Duller, H.M. Roberts, A.G. Wintle, Y.I. Lee, S.B. Yi, Dose dependence of thermally transferred optically stimulated luminescence signals in quartz, Radiat. Meas. 44 (2009) 132–143.

[16] M. Jain, A.S. Murray, L. Botter-Jensen, Characterisation of blue-light stimulated luminescence components in different quartz samples: implications for dose measurement, Radiat. Meas. 37 (2003) 441–449.

[17] B. Li, S.H. Li, Studies of thermal stability of charges associated with thermal transfer of OSL from quartz, J. Phys. D: Appl. Phys. 39 (2006) 2941–2949.

[18] B. Li, S.H. Li, Comparison of De estimates using the fast component and the medium component of quartz OSL, Radiat. Meas. 41 (2006) 125–136.

[19] B. Li, S.H. Li, A.G. Wintle, Observations of thermal transfer and the slow component of OSL signals from quartz, Radiat. Meas. 41 (2006) 639–648.

[20] S.W.S. McKeever, N. Agersnap Larsen, L. Bøtter-Jensen, V. Mejdahl, Radiat. Meas. 27 (1997) 75–82.

[21] V. Pagonis, R. Chen, A.G. Wintle, Modelling thermal transfer in optically stimulated luminescence of quartz, J. Phys. D: Appl. Phys. 40 (2007) 998–1006.

[22] V. Pagonis, A.G. Wintle, R. Chen, X.L. Wang, A theoretical model for a new dating protocol for quartz based on thermally transferred OSL (TT-OSL), Radiat. Meas. 43 (2008) 704–708.

[23] V. Pagonis, E. Balsamo, C. Barnold, K. Duling, S. McCole, Simulations of the predose technique for retrospective dosimetry and authenticity testing, Radiat. Meas. 43 (2008) 1343–1353.

[24] V. Pagonis, A.G. Wintle, R. Chen, X.L. Wang, Simulations of thermally transferred OSL experiments and of the ReSAR dating protocol for quartz, Radiat. Meas. 44 (2009) 634–638.

[25] V. Pagonis, G. Kitis, R. Chen, Applicability of the Zimmerman predose model in the thermoluminescence of predosed and annealed synthetic quartz samples, Radiat. Meas. 37 (2003) 267–274.

[26] N. Porat, G.A.T. Duller, H.M. Roberts, A.G. Wintle, A simplified SAR protocol for TT-OSL, Radiat. Meas. 44 (2009) 538–542.

[27] E.J. Rhodes, Quartz single grain OSL sensitivity distributions: implications for multiple grain single aliquot dating, Geochronometria 26 (2007) 19–29.

[28] Z.X. Shen, B. Mauz, D-e determination of quartz samples showing falling D-e(t) plots, Radiat. Meas. 44 (2009) 566–570.

[29] J.S. Singarayer, R.M. Bailey, Further investigations of the quartz optically stimulated luminescence components using linear modulation, Radiat. Meas. 37 (2003) 451–458.

[30] T. Stevens, J.P. Buylaert, A.S. Murray, Towards development of a broadly-applicable SAR TT-OSL dating protocol for quartz, Radiat. Meas. 44 (2009) 639–645.

[31] J.W. Thompson, Accuracy, precision, and irradiation time for Monte Carlo simulations of single aliquot regeneration (SAR) optically stimulated luminescence (OSL) dosimetry measurements, Radiat. Meas. 42 (2007) 1637–1646.

[32] S. Tsukamoto, G.A.T. Duller, A.G. Wintle, Characteristics of thermally transferred optically stimulated luminescence (TT-OSL) in quartz and its potential for dating sediments, Radiat. Meas. 43 (2008) 1204–1218.

[33] X.L. Wang, Y.C. Lu, A.G. Wintle, Recuperated OSL dating of .ne grained quartz in Chinese loess, Quat. Geochronol. 1 (2006) 89–100.

[34] X.L. Wang, A.G. Wintle, Y.C. Lu, Thermally transferred luminescence in fine-grained quartz from Chinese loess: basic observations, Radiat. Meas 41 (2006) 649–658.

[35] X.L. Wang, A.G. Wintle, Y.C. Lu, Testing a single-aliquot protocol for recuperated OSL dating, Radiat. Meas 42 (2007) 380–391.

[36] A.G. Wintle, A.S. Murray, A review of quartz optically stimulated luminescence characteristics and their relevance in single-aliquot regeneration dating protocols, Radiat. Meas. 41 (2006) 369–391.